

Binary radial velocity measurements with space-based gravitational-wave detectors

Kaze W.K. Wong¹, Vishal Baibhav¹, Emanuele Berti¹

¹*Department of Physics and Astronomy, Johns Hopkins University, Baltimore, MD 21218 USA*

Accepted ; Received ; in original form

ABSTRACT

Unlike traditional electromagnetic measurements, gravitational-wave observations are not affected by crowding and extinction. For this reason, compact object binaries orbiting around a massive black hole can be used as probes of the inner environment of the black hole in regions inaccessible to traditional astronomical measurements. The orbit of the binary’s barycenter around the massive black hole will cause a Doppler shift in the gravitational waveform which is in principle measurable by future space-based gravitational-wave interferometers, such as the Laser Interferometer Space Antenna (LISA). We investigate the conditions under which these Doppler shifts are observable by LISA. Our results imply that Doppler shift observations can be used to study the central region of globular clusters in the Milky Way, as well the central environment of extragalactic massive black holes.

1 INTRODUCTION

The direct detection of gravitational waves (GWs) by the LIGO/Virgo collaboration is the beginning of a new era in black hole (BH) astronomy (Abbott et al. 2018a,b) and tests of strong field gravity (Abbott et al. 2016). All GW observations so far constrained the properties of BHs (or neutron stars) in binary systems. This is in stark contrast with “traditional” astronomical BH observations, which rely on the interaction of isolated BHs with the surrounding environment, such as nearby stars (Miyoshi et al. 1995; Ghez et al. 2008; Gillessen et al. 2009) and accreting matter (Shakura & Sunyaev 1973; Peterson et al. 2004; Özel et al. 2010; Steeghs et al. 2013). By their very nature, these electromagnetic observations are subject to modelling and systematic uncertainties, weakening the supporting observational evidence for BHs and our ability to measure their parameters. For example, the very existence of intermediate-mass BHs (IMBHs) is still under debate (Kızıltan et al. 2017; Mezcua 2017).

Recent work considered various astrophysical processes, other than cosmological redshift (Markovic 1993), which may introduce measurable Doppler shifts in gravitational waveforms (Yunes et al. 2011; Gerosa & Moore 2016; Meiron et al. 2017; Inayoshi et al. 2017; Randall & Xianyu 2018a), and the astrophysical properties that could be inferred from such measurements. Doppler shift measurements in gravitational waveforms extend the class of astrophysical systems that can be studied with GW detectors beyond the strong-field merger and collapse of compact objects.

Unlike electromagnetic measurements, GW measurements do not have multiple emission lines that can be used to independently identify the Doppler shift: an event moving at constant line-of-sight velocity is degenerate with a heavier

system without proper motion (see e.g. Flanagan & Hughes 1998). For the proper motion to be detectable, we need to observe *variations* in the line-of sight velocity.

One of the most common astrophysical systems that can produce potentially detectable Doppler shifts are hierarchical triples. In the hierarchical triple scenario, the orbital period of the binary around the third body should not be too large compared to the observation period: if it is, the observed velocity of the binary will be approximately constant during the observation, hence indistinguishable from a system of different mass without proper motion. This also means that longer observation periods help us resolve larger velocity variation timescales. In contrast with Earth-based interferometers, which typically observe binary inspirals and mergers lasting for seconds or minutes, the Laser Interferometer Space Antenna (LISA) (Amaro-Seoane et al. 2017) will measure inspiral events lasting as long as a few years, and it is therefore more sensitive to Doppler shifts in the gravitational waveform.

With a few exceptions (Randall & Xianyu 2018a), most recent studies considered LISA sources where the third body has mass comparable to the GW-emitting binary (Meiron et al. 2017; Bonvin et al. 2017; Robson et al. 2018) or much smaller than the GW-emitting binary (Seto 2008; Tamanini & Danielski 2018; Steffen et al. 2018). In this work we focus on the complementary scenario where the third body is a BH of mass *much larger* than the GW-emitting binary, and we ask: how close to the BH should the GW-emitting binary be in order to yield meaningful constraints on the properties of the third body? We show that observationally interesting scenarios include (i) white dwarf binaries (WDWDs) orbiting around IMBHs, (ii) stellar-origin BH binaries (SOBHs) similar to those detected by LIGO/Virgo orbiting around

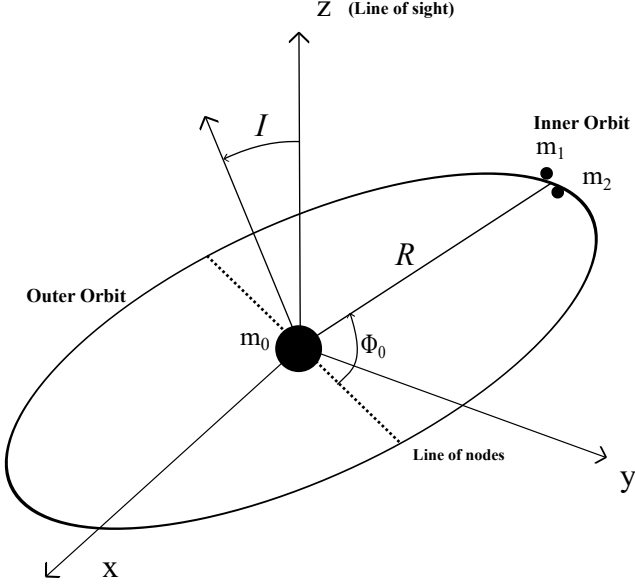


Figure 1. Illustration of the geometry of the system.

a nearby supermassive BH (SMBH) such as the one at our own galactic center, and (iii) IMBH binaries orbiting around extragalactic SMBHs.

The structure of the paper is as follows. In section 2 we describe our model for the gravitational waveform, and we review the Fisher matrix technique used in our parameter estimation calculations. In section 3 we present our main results. In section 4 we discuss the limitations of our work, their scientific implications, and directions for future work.

2 DOPPLER-SHIFTED WAVEFORM MODEL AND PARAMETER ESTIMATION

The geometry of the triple system we consider is sketched in Fig. 1. The z axis is oriented along the line of sight. The GW-emitting binary components, with masses m_1 and m_2 , are on a circular “inner” orbit; m_0 is the mass of the third body (a massive BH); I is the angle between the line of sight and the orbital angular momentum of the GW-emitting binary, whose barycenter is assumed to be on a circular “outer” orbit about the third body; R is the radius of this circular orbit. Let $M_{\text{tot}} = m_0 + m_1 + m_2$ be the total mass of the triple. We assume that the separation between the components of the inner binary is much smaller than R , i.e. that the period of the inner orbit is much shorter than the period

$$P_0 = 2\pi \sqrt{\frac{R^3}{M_{\text{tot}}}} \quad (1)$$

of the outer orbit. Under this assumption, we can model the dynamics of the inner and outer orbits separately. The line-of-sight velocity $v(t)$ for a distant observer located on the z axis is

$$v(t) = v_{\parallel} \cos\left(\frac{2\pi t}{P_0} + \Phi_0\right), \quad (2)$$

where

$$v_{\parallel} = \frac{m_0}{M_{\text{tot}}} \frac{2\pi R \sin I}{P_0} \quad (3)$$

is the magnitude of the line-of-sight velocity. The initial observed phase of the outer orbit Φ_0 is equal to zero when the GW-emitting binary is traveling along the line of sight. Here and below we use geometrical units ($G = c = 1$).

Let us now consider the effect of the Doppler modulation on the gravitational waveform. We model the non-spinning, quasicircular binary waveform by expanding the phasing up to second post-Newtonian (2PN) order, including modulations due to LISA’s orbital motion and effects due to the source location in the sky (Berti et al. 2005). In the time domain, the waveform is given by

$$h(t) = \frac{2\mathcal{M}^{5/3}}{D_L} [\pi f(t)]^{2/3} \times \frac{\sqrt{3}}{2} \tilde{A}(t) \cos \Psi_0(t), \quad (4)$$

where

$$\Psi_0(t) = 2\pi \int_0^t f(t') dt' + \varphi_p(t) + \varphi_D(t), \quad (5)$$

$f(t)$ is the GW frequency at time t in the observer frame, and D_L is the luminosity distance of the source. Here $M = m_1 + m_2$ is the observed total mass, $\eta = m_1 m_2 / M^2$ the symmetric mass ratio, and $\mathcal{M} = \eta^{3/5} M$ the chirp mass of the inner binary. The factor $\frac{\sqrt{3}}{2}$ accounts for the fact that the two independent LISA interferometer “arms” are at angles of 60° . The terms $\tilde{A}(t)$, $\varphi_p(t)$, $\varphi_D(t)$ are amplitude, polarization and Doppler-phase modulations that arise from the orbital motion of LISA, respectively. They can be expressed as functions of the binary’s orbital frequency f , sky location $(\bar{\theta}_S, \bar{\phi}_S)$ and orbital angular momentum direction $(\bar{\theta}_L, \bar{\phi}_L)$, where overbars denote quantities in the Solar System barycenter frame. Detailed expressions can be found in (Cutler 1998).

The possibility to detect cosmological effects in gravitational waveforms was discussed in great detail by Markovic (1993), while the detectability of astrophysical Doppler shifts induced by planetary systems around WDWD binaries was studied by Seto (2008). The line-of-sight velocity changes the observer-frame frequency of the source through a Doppler shift $f_O = f_S(1 + v)$. This results into an additional phasing term in the waveform: $\Psi_0(t) \rightarrow \Psi_0(t) + \phi_{\text{pm}}(t)$ (Seto 2008; Bonvin et al. 2017; Inayoshi et al. 2017; Randall & Xianyu 2018a; Robson et al. 2018), where the proper-motion modulation $\phi_{\text{pm}}(t)$ is related to the velocity profile $v(t)$ of Eq. (2) by

$$\phi_{\text{pm}}(t) = 2\pi \int_0^t v(t') f(t') dt'. \quad (6)$$

If we omit the effect of proper motion in the analysis of LISA data this phase shift will appear as a residual, which contains information on the properties of the outer orbit.

Our waveform model depends on 12 parameters, which we will denote collectively as $\theta = \{\theta_i\}$. Nine of these parameters – i.e. $\{D_L, \mathcal{M}, \eta, t_c, \phi_c, \bar{\theta}_S, \bar{\theta}_L, \bar{\phi}_S, \bar{\phi}_L\}$, where t_c and ϕ_c are the coalescence time and phase (Poisson & Will 1995), respectively – characterize the inner binary; the remaining three parameters $\{v_{\parallel}, P_0, \Phi_0\}$ characterize the outer orbit. Sampling the entire 12-dimensional parameter space is computationally expensive. To estimate whether the outer orbit

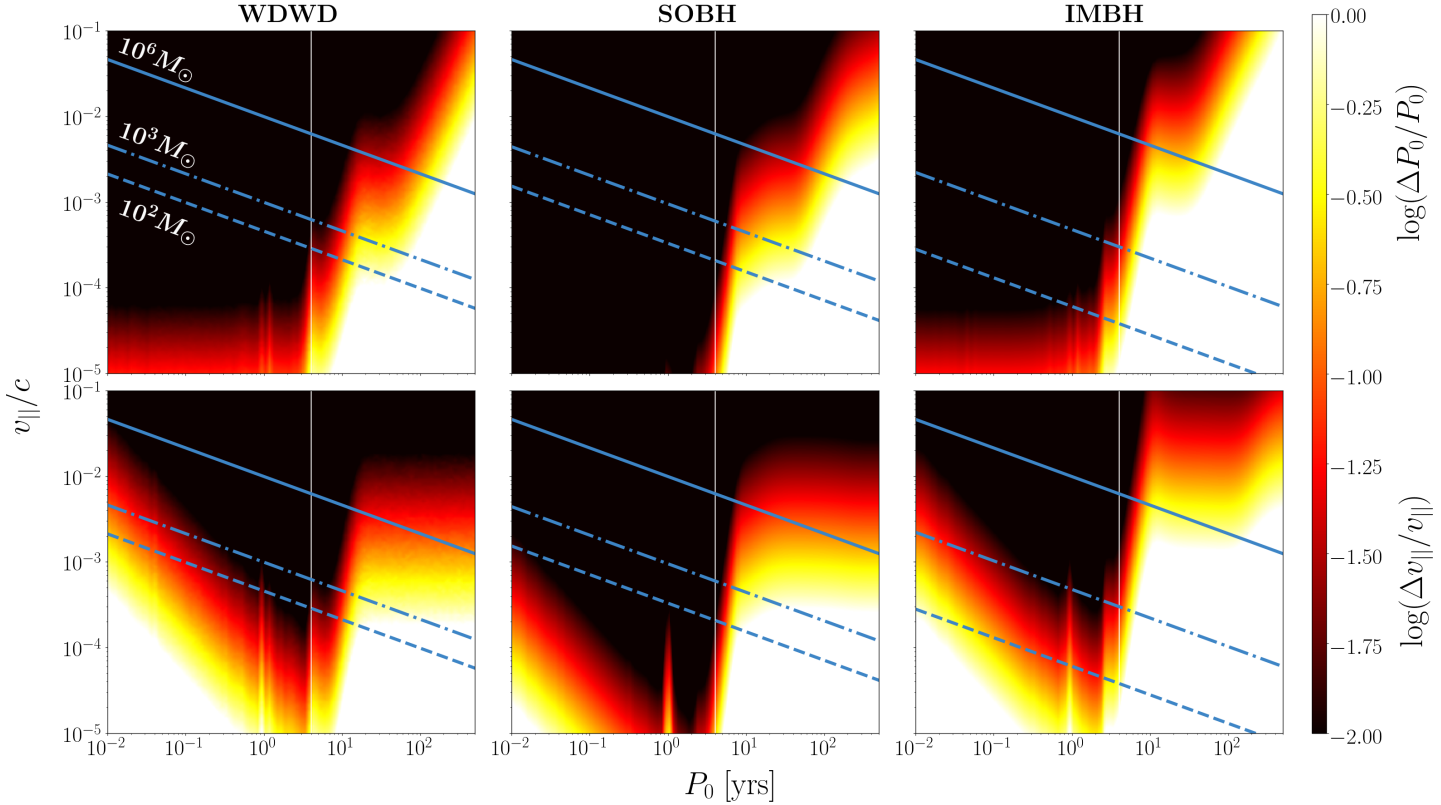


Figure 2. Contour plots of the logarithmic relative error in the orbital period P_0 (top row) and magnitude of the line-of-sight velocity $v_{||}$ (bottom row) in the $(P_0, v_{||})$ plane. The three columns correspond to our three chosen physical systems at fixed SNR $\rho = 10$: WDWD at 10^{-3} Hz (left), SOBH (middle) and IMBH (right). In the regions above the solid, dash-dotted and dashed lines the third body must have mass larger than $10^6 M_\odot$, $10^3 M_\odot$ and $10^2 M_\odot$, respectively, to produce the observed Doppler shift. The vertical white line corresponds to the nominal LISA mission lifetime $T_{\text{obs}} = 4$ yr.

parameters responsible for the Doppler modulation are measurable we use a Fisher matrix analysis (Berti et al. 2005). For a source with signal-to-noise ratio (SNR) ρ , defined in terms of the LISA one-sided spectral density $S_n(f)$ as

$$\rho^2 = 2 \sum_{\alpha=I,II} \int_0^{T_{\text{obs}}} dt \frac{|h_\alpha(t)|^2}{S_n(f(t))}, \quad (7)$$

in the large-SNR approximation the uncertainties in the source parameters are inversely proportional to ρ : $\Delta\theta^i \propto 1/\rho$. These uncertainties are given by the diagonal terms of the covariance matrix Σ : $\Delta\theta^i = \sqrt{\Sigma_{ii}}$ where $\Sigma = \Gamma^{-1}$ is the inverse of the Fisher information matrix, with elements

$$\Gamma_{ij} \equiv 2 \sum_{\alpha=I,II} \int_0^{T_{\text{obs}}} dt \frac{\partial h_\alpha(t)}{\partial \theta^i} \frac{\partial h_\alpha(t)}{\partial \theta^j} \frac{1}{S_n(f(t))}. \quad (8)$$

Here T_{obs} is the observation time, and α labels the two independent LISA data channels.

3 RESULTS

Sampling over the 12-dimensional parameter space is computationally expensive, so we consider three specific examples to determine typical conditions under which Doppler modulations may be detectable by LISA:

Table 1. Luminosity distance for the three source classes considered in this paper.

ρ	WDWD	SOBH	IMBH
10	1.40 kpc	178 Mpc	5720 Mpc
100	0.140 kpc	16.9 Mpc	679 Mpc

- (i) a $0.6\text{--}0.6 M_\odot$ WDWD binary with a source-frame GW frequency 10^{-3} Hz;
- (ii) a GW150914-like $36\text{--}29 M_\odot$ SOBH binary inspiral starting 5 yr before merger;
- (iii) a $10^3\text{--}10^3 M_\odot$ IMBH binary inspiral starting 5 yr before merger.

All masses listed above are in the source frame. We consider an observation time $T_{\text{obs}} = 4$ yr, corresponding to the nominal LISA mission lifetime (Audley et al. 2017). We place the sources at a luminosity distance such that the two-detector LISA SNR is either $\rho = 10$ or $\rho = 100$. For convenience, these luminosity distances are listed in Table 1. For simplicity we set $t_c = \phi_c = 0$ and we choose the orientation parameters to be $\{\bar{\theta}_S, \bar{\theta}_L, \bar{\phi}_S, \bar{\phi}_L\} = \{\arccos(0.3), \arccos(-0.2), 5, 4\}$ for all three sources. We have verified that our choice of orientation parameters does not significantly affect our conclusions (it mainly affects the measurement accuracy by a rescaling of the SNR).

We sample over the outer binary parameters $v_{||}$ and P_0 within the range $v_{||}/c \in [10^{-5}, 10^{-1}]$ and $P_0 \in [10^{-2}, 500]$ yr. If $P_0 < T_{\text{obs}}$ the choice of the outer initial orbital phase Φ_0 does not significantly affect the measurement, since we can measure a whole modulation cycle from the outer orbit, and therefore we set $\Phi_0 = 0$. If instead $P_0 > T_{\text{obs}}$ the choice of Φ_0 can affect the uncertainties and correlations between parameters. We postpone a more detailed investigation of this regime to future work. For computational efficiency we compute parameter estimation uncertainties following the frequency-domain method of [Chamberlain et al. \(2018\)](#) for inspiralling binaries (SOBH and IMBH), while we use the time-domain procedure described in Sec. 2 for WDWD binaries, where the inspiral is negligible.

Figure 2 shows uncertainties in $v_{||}$ and P_0 as a function of the simulated $v_{||}$ and P_0 . On the left of each of the panels, $P_0 < T_{\text{obs}}$, and the correlation between the parameters of interest is small. In this case $f(t)$ is approximately constant, so we can pull it out of the integral in Eq. (6) to find

$$\phi_{\text{pm}} = \frac{v_{||} P_0}{2\pi} \sin\left(\frac{2\pi t}{P_0} + \Phi_0\right). \quad (9)$$

Then, ignoring correlations between parameters, the fractional uncertainty on $v_{||}$ and P_0 scales as

$$\frac{\Delta v_{||}}{v_{||}} \propto \sqrt{(\Gamma^{-1})_{v_{||} v_{||}}} \frac{1}{v_{||}} \propto \frac{1}{\rho v_{||} P_0}, \quad (10a)$$

$$\frac{\Delta P_0}{P_0} \propto \sqrt{(\Gamma^{-1})_{P_0 P_0}} \frac{1}{P_0} \propto \frac{1}{\rho v_{||}}. \quad (10b)$$

This is consistent with the behavior observed in Figure 2. The spike in the uncertainty on $v_{||}$ occurs when $P_0 \sim 1$ yr: in this case the Doppler modulation due to the motion of the source is hard to measure because it is degenerate with the Doppler phase from the motion of the LISA detector (cf. [Tamanini & Danielski 2018](#)).

Just as in electromagnetic measurements based on the radial velocity method, the observed velocity profile is completely degenerate with inclination. Eq. (3) can be rewritten as

$$\frac{m_0 R \sin I}{M_{\text{tot}}} = \frac{P_0 v_{||}}{2\pi}. \quad (11)$$

Therefore R and $\sin I$ (or m_0 and $\sin I$) cannot be measured independently from Doppler shift measurements of $v_{||}$ and P_0 . For any given measurement of $(v_{||}, P_0)$ we can still place a lower bound on m_0 (and a corresponding upper bound on R) by setting $\sin I = 1$. The blue lines in Figure 2 map the measured values of $v_{||}$ and P_0 to the minimum mass of the third body m_0^{min} necessary to produce the observed Doppler shift using Eq. (3). For example, if we measure a signal consistent with $v_{||} = 10^{-2}c$ and $P_0 = 2$ years, the third body must have mass $m_0 > m_0^{\text{min}} \sim 10^3 M_{\odot}$.

While in Figure 2 we characterized our ability to observe the binary’s proper motion in terms of the observables $v_{||}$ and P_0 , from an astrophysical standpoint it is more useful to use the mass of the third body m_0 and the outer orbital radius R . We can translate the results on the observability of the Doppler shift in the $(v_{||}, P_0)$ plane (Figure 2) to criteria for the observability of the Doppler shift in the $(m_0, R \sin I)$ plane, as shown in Figure 3. The shaded regions in this plot are not sampled in our parameter estimation survey for one of the following reasons: the period P_0 is too long ($P_0 >$

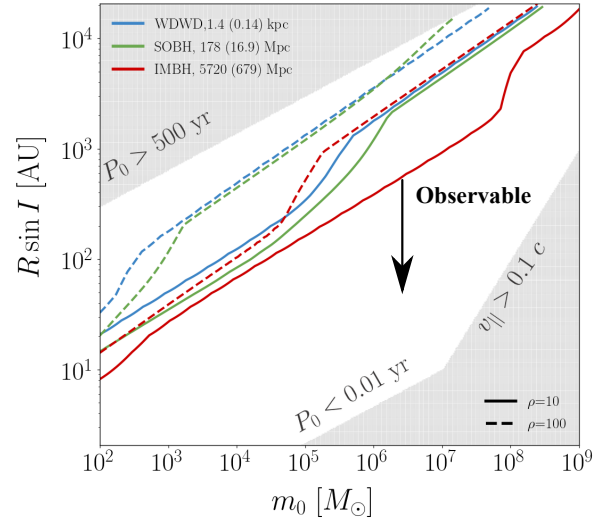


Figure 3. Region in the $(m_0, R \sin I)$ plane where the Doppler shift is observable: below each of the representative lines in this plot *both* P_0 and $v_{||}$ are measured to better than 10% uncertainty. The blue, green and red lines correspond to WDWD, SOBH and IMBH inner binaries, respectively. The solid lines refer to binaries that are barely detectable ($\rho = 10$); the corresponding luminosity distances are given in Table 1 and in the legend. The dashed lines refer to loud detections with $\rho = 100$. The shaded regions were not sampled in our parameter estimation calculations (see the text).

500 yr, upper-left shaded triangle), too short ($P_0 < 0.01$ yr, bottom-right), or the magnitude of the line-of-sight velocity $v_{||} > 0.1$, so that the nonrelativistic approximation becomes unreliable.

The solid and dashed lines show how close the inner binary can be to a third body of mass m_0 for the proper motion Doppler signature to be observable: below those lines, fractional uncertainties in *both* $v_{||}$ and P_0 are smaller than 10% for binary signals with SNR $\rho = 10$ (solid lines) or $\rho = 100$ (dashed lines). The “bumps” in each of the solid and dashed lines correspond to the slight plateau in the uncertainty on P_0 in the high- P_0 regime (cf. the upper row of Figure 2). For astrophysical purposes, it is more useful to translate these SNR values into the horizon distances listed in Table 1 and to keep in mind that the source SNR is inversely proportional to the luminosity distance (at least for binaries in the local universe, such as WDWDs, where cosmological effects are negligible). Recall also that for sources at distances where cosmological effects are non-negligible (SOBHs and IMBHs) the observed chirp mass of the source is redshifted to $(1+z)\mathcal{M}$ ([Markovic 1993](#); [Flanagan & Hughes 1998](#)).

While we considered a wide range of possible values for m_0 and $R \sin I$, it is clear from Table 1 that the three source classes are of interest in different astrophysical scenarios. WDWD systems can be detected by LISA within a few kpc, and their Doppler modulation could be used to identify IMBHs in nearby stellar clusters. SOBHs can be detected within ~ 200 Mpc, and their Doppler modulation could be used to probe the center of nearby galaxies at $z \lesssim 0.05$. IMBHs can be detected out to ~ 6 Gpc, so Doppler modulations could be used to study galaxy forma-

tion out to redshifts $z \sim 1$. Note that the horizon distance of the source has a strong dependence on the inner binary mass and sky location (which were fixed in our study for computational reasons), therefore the numbers quoted above should be considered as illustrative for each astrophysical scenario, rather than as rigorous detection limits.

4 DISCUSSION

This study is a proof-of-principle investigation of the conditions under which Doppler shifts in gravitational waveforms could be measurable by LISA.

Our analysis differs in several ways from recent work by Inayoshi et al. (2017) and Bonvin et al. (2017). Inayoshi et al. (2017) carry out a Fisher matrix analysis using a six-parameter model, including chirp mass, symmetric mass ratio, distance, time and phase of coalescence and an acceleration parameter Y . They do not account for LISA's orbital motion and the source orientation, while we do. This is crucial: the measurability of Doppler effects depends on the relative magnitude of the orbital period of the source with respect to LISA's orbital period. There are features (most notably the spike in uncertainties when the period of the outer orbit is close to 1 yr) that can only be accounted for when LISA's motion is considered. Besides, ignoring degeneracies (e.g. between the inclination of the source and the chirp mass) can lead to overly optimistic parameter estimation. Another important difference is that the acceleration parameter Y used in Inayoshi et al. (2017) is a linear approximation of the phase shift we considered here, so their phase shift is linear in time: see e.g. their Eq. (7). This corresponds to a special case of our analysis: the long-period regime. In this regime the correlation between the velocity of the source and the period of the outer orbit is important, but it was ignored in Inayoshi et al. (2017). Besides, a measurement of their parameter Y cannot be translated into a measurement of the third body's mass and of the orbital radius of the binary R around the third body: at least one more variable is needed to get a lower bound on the mass of the third body.

Bonvin et al. (2017) and Inayoshi et al. (2017) consider mostly SOBHs as gravitational-wave sources, while we also considered WDWD binaries and IMBH binaries. As we show in our work, the detectability of Doppler effects depends dramatically on the choice of source. Besides, both Inayoshi et al. (2017) and Bonvin et al. (2017) focus on the acceleration effect. The values of the ϵ parameter introduced in Eq. (51) of Bonvin et al. (2017) correspond to orbital periods $\gtrsim 10^4$ yr, well beyond the range considered in our study.

In this exploratory study we have made simplifying assumptions that we discuss below, and that should be relaxed in more realistic scenarios.

The assumption of a circular outer orbit can be considered conservative, because eccentricity in the outer orbit makes Doppler shifts easier to observe (Robson et al. 2018). In general, there will be a trade-off between the detectability gain due to large variations in $v_{||}$ near pericenter and the fact that (because of Kepler's second law) it is statistically more likely to find astrophysical systems near apocenter. The distribution of the outer and inner orbital eccentricities plays an important role when computing rates of LISA

events with observable Doppler shifts (Nishizawa et al. 2016; Breivik et al. 2016; Randall & Xianyu 2018b,c,a; Samsing & D'Orazio 2018; D'Orazio & Samsing 2018; Rodriguez et al. 2018; Nishizawa et al. 2017), and we plan to address this issue in future work.

We modelled the outer orbit using Newtonian dynamics. This should be sufficient for most astrophysical systems of interest: the dominant corrections to the equations of motion enter at order $(v/c)^2$, and therefore they should be mostly negligible even for $v_{||} \sim 0.1c$. Furthermore, the dominant post-Newtonian correction increases the orbital period (see e.g. Poisson & Will 2014), hence it improves the observability bounds shown in Figure 3 for given orbital parameters. In this sense, once again, our predictions are conservative.

In principle we can convolve the Doppler observability criteria shown in Figure 3 with astrophysical models to predict the number of events for which LISA will be able to observe Doppler shifts. Vice versa, we could use LISA observations of Doppler shifts (or the lack thereof) to constrain astrophysical models. A detailed discussion of the astrophysical implications of our results is beyond the scope of this paper. In the hope to stimulate further research, we briefly discuss some astrophysical scenarios that could lead to observable Doppler shifts for the three source classes considered in this paper: WDWD, SOBH and IMBH binaries.

(i) **WDWDs:** WDWD systems can be detected by LISA within a few kpc, and their Doppler modulation could be used to identify IMBHs in nearby stellar clusters. There is a broad range of estimates of the number of binaries detectable by LISA in Milky Way globular clusters, with some of the latest estimates ranging from a few to tens of events (Kremer et al. 2018). The uncertainties are dominated by assumptions on cluster models, such as the binary fraction (Ivanova et al. 2005; Sollima et al. 2007; Hurley et al. 2007; Albrow et al. 2001) and the efficiency of different dynamical processes (Hénon 1971; Amaro-Seoane & Spurzem 2001; Fregeau et al. 2004). The number of WDWD events with an observable proper motion signature in LISA could be used to set constraints on these cluster models.

(ii) **SOBHs:** SOBHs can be detected by LISA within ~ 200 Mpc, and their Doppler modulation could be used to probe the center of nearby galaxies at $z \lesssim 0.05$. The LIGO/Virgo collaboration has already detected 10 BH-BH binary mergers (Abbott et al. 2018a), and yet there is no consensus on the astrophysical origin of these mergers (Abbott et al. 2018b). One possibility is that these compact binaries are formed in the vicinity of AGNs (see e.g. Fragione et al. 2018a). Indeed, the presence of X-ray binaries (Hailey et al. 2018) and hypervelocity stars (Brown et al. 2005; Sherwin et al. 2008) close to our galactic center indicates that a large number of binaries exist in galactic nuclei. Gaseous drags or three-body interactions in AGN disks can lead to very hard binaries that should coalesce within a Hubble time (Stone et al. 2017). Hoang et al. (2018) showed that the merger rates of such binaries could be comparable to other dynamical channels. The merger process is very efficient if these binaries lie within ~ 0.1 pc, resulting in a significant fraction of mergers happening very close to the SMBH. Furthermore, compact objects embedded in AGN disks create density perturbations, resulting in torques that lead to inward migration of the compact object. Sometimes this torque changes sign, leading to the formation of migra-

tion traps at $40M-600M$ from the central objects (Bellovary et al. 2016) which could act as hotbeds for the formation of BH-BH binaries. In summary, there are various scenarios that could lead to SOBH binaries merging very close to an SMBH. These systems may have detectable Doppler shifts that could serve as smoking guns for binary formation in AGNs. It is even possible that SMBH mass measurements from Doppler-shifted GWs could complement and/or improve electromagnetic estimates of the AGN mass.

Another interesting scenario was proposed by Han & Chen (2018) and Chen & Han (2018). These authors proposed that some extreme mass-ratio inspirals (EMRIs) could actually be *binary* BH systems inspiralling into a supermassive BHs. These “binary EMRIs” (or b-EMRIs) source GWs both through the motion of the inner BH-BH binary and through the inspiral of the b-EMRI. If such sources exist, the Doppler shift in the GWs from the BH-BH binary could allow us to estimate the SMBH mass. The Doppler-shift estimate of the central SMBH mass could be used as an independent check of the parameters estimated using the gravitational radiation from the b-EMRI inspiral.

(iii) **IMBHs:** IMBH binaries can be detected by LISA out to a few Gpc, so Doppler modulations could be used to study galaxy formation out to redshifts $z \sim 1$. Despite claims of a connection between IMBHs and ultra-luminous X-ray sources (Colbert & Mushotzky 1999) and other observational evidence (Caballero-Garcia et al. 2013; Pasham et al. 2015; Chilingarian et al. 2018; Nguyen et al. 2019), there is still no conclusive observational confirmation of the existence of IMBHs (see e.g. Mezcua 2017, for a review). IMBH detections could bridge the gap between SOBHs and SMBHs, and help us understand how SMBH were born and grew. In some scenarios, clusters containing IMBHs sink towards the galactic nucleus through dynamical friction, and upon evaporation deposit their IMBHs near the galactic center (Ebisuzaki et al. 2001). The IMBHs then form binaries and eventually merge, forming an SMBH. Some of these IMBH binaries could end up in orbit around a more massive central object (Fragione et al. 2018b,c), and orbital Doppler shifts could lead to biases in their estimated masses (Arca-Sedda & Gualandris 2018; Arca-Sedda & Capuzzo-Dolcetta 2019). GW detections of these systems by Earth- or space-based interferometers could provide conclusive evidence of SMBH formation through runaway IMBH collisions.

In conclusion, several astrophysical GW sources are expected to form triple systems where the main GW emission from an “inner” orbit is affected by Doppler modulations due to the “outer” orbital motion of the binary around a third body. LISA (unlike ground based detectors) may observe the radiation from the inner binary for months or years. GW searches and parameter estimation methods rely on waveform modelling, so failure to account for Doppler modulations could introduce systematics in parameter estimation and reduce the efficiency of GW searches (Bonvin et al. 2017). In this paper we argued that, more interestingly, these effects may be observable, enabling GW detectors to probe weak-field astrophysical processes through the Doppler modulations of their strong-field inspiral dynamics. We investigated the conditions under which LISA may place meaningful constraints on the third body’s properties, and we identified and discussed some classes of astrophysical systems of particular interest as observational targets.

We plan to extend the present research in two main directions: (i) by developing more realistic (and complex) possibilities for the orbital motion and GW emission of the triples, and (ii) by using astrophysical models to identify the most promising astrophysical systems that could lead to LISA detections of Doppler modulations.

ACKNOWLEDGMENTS

We thank Nicola Tamanini, Davide Gerosa, Hsiang-Chih Hwang, Tyson Littenberg, Christopher Moore, Lisa Randall, Travis Robson and Nadia Zakamska for useful discussions. K.W.K.W., V.B. and E.B. are supported by NSF Grant No. PHY-1841464, NSF Grant No. AST-1841358, NSF-XSEDE Grant No. PHY-090003, and NASA ATP Grant No. 17-ATP17-0225. This research project received funding from the European Union’s Horizon 2020 research and innovation programme under the Marie Skłodowska-Curie grant agreement No. 690904, and it used computational resources at the Maryland Advanced Research Computing Center (MARCC). The authors would like to acknowledge networking support by the GWverse COST Action CA16104, “Black holes, gravitational waves and fundamental physics.”

REFERENCES

- Abbott B. P., et al., 2016, *Physical Review Letters*, **116**, 221101
- Abbott B. P., et al., 2018a, preprint ([arXiv:1811.12940](#))
- Abbott B. P., et al., 2018b, preprint ([arXiv:1811.12907](#))
- Albrow M. D., Gilliland R. L., Brown T. M., Edmonds P. D., Guhathakurta P., Sarajedini A., 2001, *Astrophys. J.*, **559**, 1060
- Amaro-Seoane P., Spurzem R., 2001, *Mon. Not. Roy. Astron. Soc.*, **327**, 995
- Amaro-Seoane P., et al., 2017, preprint, ([arXiv:1702.00786](#))
- Arca-Sedda M., Capuzzo-Dolcetta R., 2019, *MNRAS*, **483**, 152
- Arca-Sedda M., Gualandris A., 2018, *MNRAS*, **477**, 4423
- Audley H., et al., 2017, preprint ([arXiv:1702.00786](#))
- Bellovary J. M., Mac Low M.-M., McKernan B., Ford K. E. S., 2016, *Astrophys. J.*, **819**, L17
- Berti E., Buonanno A., Will C. M., 2005, *Phys. Rev.*, **D71**, 084025
- Bonvin C., Caprini C., Sturani R., Tamanini N., 2017, *Phys. Rev.*, **D95**, 044029
- Breivik K., Rodriguez C. L., Larson S. L., Kalogera V., Rasio F. A., 2016, *Astrophys. J.*, **830**, L18
- Brown W. R., Geller M. J., Kenyon S. J., Kurtz M. J., 2005, *Astrophys. J.*, **622**, L33
- Caballero-Garcia M. D., Belloni T., Zampieri L., 2013, *Mon. Not. Roy. Astron. Soc.*, **436**, 3262
- Chamberlain K., Moore C. J., Gerosa D., Yunes N., 2018, preprint ([arXiv:1809.04799](#))
- Chen X., Han W.-B., 2018, *Communications Physics*, **1**, 53
- Chilingarian I. V., Katkov I. Y., Zolotukhin I. Y., Grishin K. A., Beletsky Y., Boutsia K., Osip D. J., 2018, *ApJ*, **863**, 1
- Colbert E. J. M., Mushotzky R. F., 1999, *Astrophys. J.*, **519**, 89
- Cutler C., 1998, *Phys. Rev.*, **D57**, 7089
- D’Orazio D. J., Samsing J., 2018, *Mon. Not. Roy. Astron. Soc.*, **481**, 4775
- Ebisuzaki T., et al., 2001, *Astrophys. J.*, **562**, L19
- Flanagan E. E., Hughes S. A., 1998, *Phys. Rev.*, **D57**, 4535
- Fragione G., Grishin E., Leigh N. W. C., Perets H. B., Perna R., 2018a, preprint, ([arXiv:1811.10627](#))
- Fragione G., Ginsburg I., Kocsis B., 2018b, *ApJ*, **856**, 92

- Fragione G., Leigh N. W. C., Ginsburg I., Kocsis B., 2018c, *ApJ*, **867**, 119
- Fregeau J. M., Cheung P., Portegies Zwart S. F., Rasio F. A., 2004, *Mon. Not. Roy. Astron. Soc.*, **352**, 1
- Gerosa D., Moore C. J., 2016, *Phys. Rev. Lett.*, **117**, 011101
- Ghez A. M., et al., 2008, *Astrophys. J.*, **689**, 1044
- Gillessen S., Eisenhauer F., Trippe S., Alexander T., Genzel R., Martins F., Ott T., 2009, *Astrophys. J.*, **692**, 1075
- Hailey C. J., Mori K., Bauer F. E., Berkowitz M. E., Hong J., Hord B. J., 2018, *Nature*, **556**, 70 EP
- Han W.-B., Chen X., 2018, preprint ([arXiv:1801.07060](https://arxiv.org/abs/1801.07060))
- H  non M., 1971, *Astrophysics and Space Science*, **13**, 284
- Hoang B.-M., Naoz S., Kocsis B., Rasio F. A., Dosopoulou F., 2018, *Astrophys. J.*, **856**, 140
- Hurley J. R., Aarseth S. J., Shara M. M., 2007, *Astrophys. J.*, **665**, 707
- Inayoshi K., Tamanini N., Caprini C., Haiman Z., 2017, *Phys. Rev.*, **D96**, 063014
- Ivanova N., Belczynski K., Fregeau J. M., Rasio F. A., 2005, *Mon. Not. Roy. Astron. Soc.*, **358**, 572
- Kiziltan B., Baumgardt H., Loeb A., 2017, *Nature*, **542**, 203
- Kremer K., Chatterjee S., Breivik K., Rodriguez C. L., Larson S. L., Rasio F. A., 2018, *Phys. Rev. Lett.*, **120**, 191103
- Markovic D., 1993, *Phys. Rev.*, **D48**, 4738
- Meiron Y., Kocsis B., Loeb A., 2017, *Astrophys. J.*, **834**, 200
- Mezcua M., 2017, *International Journal of Modern Physics D*, **26**, 1730021
- Miyoshi M., Moran J., Herrnstein J., Greenhill L., Nakai N., Diamond P., Inoue M., 1995, *Nature*, **373**, 127
- Nguyen D. D., et al., 2019, preprint, ([arXiv:1901.05496](https://arxiv.org/abs/1901.05496))
- Nishizawa A., Berti E., Klein A., Sesana A., 2016, *Phys. Rev.*, **D94**, 064020
- Nishizawa A., Sesana A., Berti E., Klein A., 2017, *Mon. Not. Roy. Astron. Soc.*, **465**, 4375
-   zel F., Psaltis D., Narayan R., McClintock J. E., 2010, *ApJ*, **725**, 1918
- Pasham D. R., Strohmer T. E., Mushotzky R. F., 2015, preprint ([arXiv:1501.03180](https://arxiv.org/abs/1501.03180))
- Peterson B. M., et al., 2004, *Astrophys. J.*, **613**, 682
- Poisson E., Will C. M., 1995, *Phys. Rev.*, **D52**, 848
- Poisson E., Will C. M., 2014, *Gravity*. Cambridge University Press
- Randall L., Xianyu Z.-Z., 2018a, preprint ([arXiv:1805.05335](https://arxiv.org/abs/1805.05335))
- Randall L., Xianyu Z.-Z., 2018b, *Astrophys. J.*, **853**, 93
- Randall L., Xianyu Z.-Z., 2018c, *Astrophys. J.*, **864**, 134
- Robson T., Cornish N. J., Tamanini N., Toonen S., 2018, *Phys. Rev.*, **D98**, 064012
- Rodriguez C. L., Amaro-Seoane P., Chatterjee S., Kremer K., Rasio F. A., Samsing J., Ye C. S., Zevin M., 2018, *Phys. Rev.*, **D98**, 123005
- Samsing J., D’Orazio D. J., 2018, *Mon. Not. Roy. Astron. Soc.*, **481**, 5445
- Seto N., 2008, *Astrophys. J.*, **677**, L55
- Shakura N. I., Sunyaev R. A., 1973, *Astron. Astrophys.*, **24**, 337
- Sherwin B. D., Loeb A., O’Leary R. M., 2008, *Mon. Not. Roy. Astron. Soc.*, **386**, 1179
- Sollima A., Beccari G., Ferraro F. R., Fusi Pecci F., Sarajedini A., 2007, *Mon. Not. Roy. Astron. Soc.*, **380**, 781
- Steeghs D., McClintock J. E., Parsons S. G., Reid M. J., Littlefair S., Dhillon V. S., 2013, *Astrophys. J.*, **768**, 185
- Steffen J. H., Wu D.-H., Larson S. L., 2018, preprint ([arXiv:1812.03438](https://arxiv.org/abs/1812.03438))
- Stone N. C., Metzger B. D., Haiman Z., 2017, *Mon. Not. Roy. Astron. Soc.*, **464**, 946
- Tamanini N., Danielski C., 2018, preprint ([arXiv:1812.04330](https://arxiv.org/abs/1812.04330))
- Yunes N., Coleman Miller M., Thornburg J., 2011, *Phys. Rev.*, **D83**, 044030